

PACS numbers: 42.55.Mv; 33.20.Kf; 33.50.Dq
DOI: 10.1070/QE2009v039n08ABEH013985

Influence of absorption from excited singlet states on the lasing parameters of polymethine dyes

V.A. Svetlichnyi, O.K. Bazyl', E.R. Kashapova, N.A. Derevyanko, A.A. Ishchenko

***Abstract*. The influence of absorption from excited singlet states (singlet – singlet absorption) on the lasing parameters of ionic (symmetric and asymmetric cationic) and intraionic (merocyanine) polymethine dyes excited by nanosecond 532-nm second-harmonic pulses from a Nd : YAG laser and 308-nm pulses from a XeCl laser is studied. It is shown that singlet – singlet absorption at the pump and lasing wavelengths affects the spectral and energy lasing parameters of organic dye solutions.**

Keywords: *cationic and intraionic polymethine dyes, electronic structure, absorption, luminescence and lasing properties, far red range, excited-state absorption.*

1. Introduction

Tunable dye lasers have already been used in optical technologies over 40 years. In the last decades, the scope of their applications became somewhat narrower due to the development of parametrically tunable lasers, tunable Ti^{3+} : sapphire lasers and some other types of lasers. The main disadvantages of pulsed dye lasers, which reduce their competitiveness, are the use of liquid solutions as active media and the photodecomposition of dyes during their operation. The attempts to use solid active media such as polymers, porous glasses, etc. doped with laser dyes, despite the achievement of lasing parameters compared to these inherent in liquid solutions, have not found commercial applications so far. Nevertheless, because there exist many efficient laser dyes producing readily tunable laser emission upon pulse pumping, dye lasers are still used both in scientific studies, for example, in spectroscopy and for a number of practical applications in medicine, for remote atmosphere probing, and laser isotope separation [1 – 3].

The search for efficient and stable laser dyes emitting in the blue ($\sim$ 400 nm) and red (700 – 800 nm) regions and the investigation of photoprocesses in laser dyes affecting their lasing parameters upon high-power pulse pumping remains of current interest. One of the factors affecting the lasing efficiency of organic dyes is the excited-state absorption. Triplet – triplet absorption and its influence on the lasing properties of many laser dyes is studied quite completely [4] because the presence of even weak singlet – triplet conversion and weak triplet – triplet absorption often noticeably reduce the lasing efficiency. Considerably less attention has been given to the study of the influence of the $S_1 \rightarrow S_n$ absorption of the lasing parameters of dyes. However, the presence of the intense $S_1 \rightarrow S_n$ absorption bands also can strongly affect the lasing parameters of organic dyes.

In this paper, we studied experimentally and theoretically (quantum-chemically) excited-state singlet – singlet absorption in three polymethine dyes: cationic electronically asymmetric (1) and intraionic (merocyanine) (2) compared to the known symmetric cationic dye (3) presented in a dye catalogue as HITC. We investigated the influence of the $S_1 \rightarrow S_n$ absorption on the lasing parameters of these dyes pumped by nanosecond pulses.

2. Objects and experimental methods

Figure 1 presents the structural formulas of dyes 1 – 3 [5 – 6] containing an indolinylidene fragment as one of the end groups. This is rather convenient for studying excited-state absorption, because this absorption is often caused by transitions localised at end groups. In addition, dyes 1 and 3 have the same cationic nature with the total chromophore charge +1 and the same length of the polymethine chain. Asymmetric dye 1 contains two different end fragments, while symmetric dye 3 has two identical fragments. In dye 1, a positive charge is mainly localised on an electric donor 1,3-diphenyl benzimidasole fragment in the ground state. This causes a considerable alternation of single and double bonds in the polymethine chain. In the first case, intermolecular interactions with a medium are enhanced, and in the second one – vibronic interactions in a molecule [5]. Both these factors cause a considerable broadening of absorption bands compared to the bands of its symmetric analogue 3. Intraionic merocyanine 2 also belongs to asymmetric polymethines, however, its chromophore is electrically neutral. The electronic structure of dye 2 in the ground state is close to that of neutral polyene with strongly alternating single and double bonds. As a result, this dye, as cationic dye 1, has a broad absorption band. A change in the solvent polarity causes opposite effects in the absorption spectra of dyes 1 and 2. As the solvent polarity is increased, the absorption band of dye 1 broadens and

V.A. Svetlichnyi, O.K. Bazyl', E.R. Kashapova V.D. Kuznetsov Siberian Physical-Technical Institute, Tomsk State University, pl. Novosobornaya 1, 634050 Tomsk, Russia; e-mail: svet@spti.tsu.ru;
N.A. Derevyanko, A.A. Ishchenko Institute of Organic Chemistry, National Academy of Sciences of Ukraine, Murmanskaya 5, 02094 Kiev, Ukraine; e-mail: alexish@i.com.ua

Received 1 October 2008; revision received 28 January 2009
Kvantovaya Elektronika **39** (8) 739 – 744 (2009)
Translated by M.N. Sapozhnikov

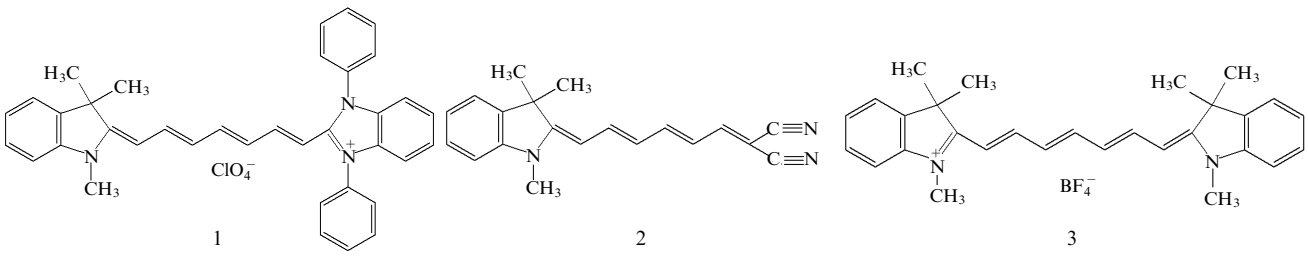

Figure 1. Structural formulas of polymethine dyes under study.

experiences the hypsochromic shift (negative solvatochromism), whereas the absorption band of dye 2 narrows down and experiences the bathochromic shift (positive solvatochromism).

Despite the different ionic nature of cationic (1) [5] and intraionic (2) [6] dyes, their electronic structures in the excited state are similar to that of symmetric polymethines. Because of this, they exhibit narrow fluorescence bands. The electronic structures of dyes 1 and 2 in the ground and excited states are considerably different. As a result, the Stokes shift observed in their spectra is considerably greater than that for symmetric dye 3, for which the electronic structures in the ground and excited states are similar [5]. The large Stokes shifts and broad absorption bands of dyes 1 and 2 make then attractive for using as active media in lasers. The large Stokes shift provides a strong red shift of the laser emission band with respect to the pump frequency and weak reabsorption, while the broad absorption band ensures efficient pumping by various pump sources.

We studied the absorption and luminescence properties of dye solutions at concentrations $10^{-6} - 10^{-4}$ M and their lasing properties – at concentrations $2 \times 10^{-4} - 2 \times 10^{-3}$ M. The solvent was propylene carbonate (PC) of extra high purity, which was used without additional purification. This solvent provided the highest lasing efficiency for all the dyes under study, which is caused by its high polarity and viscosity [5]. The high polarity leads to a considerable increase in the solubility of dyes 1 – 3, providing high optical densities at the pump frequencies, and excludes the formation of ionic pairs and associates of salt-like dyes 1 and 3, which causes fluorescence quenching [5]. The high viscosity of the solvent provides an increase in the quantum yield of fluorescence of all the dyes under study due to the retardation of rotation around the polymethine chain. It is photoisomerisation that causes the efficient nonradiative deactivation of the excited states of polymethine dyes [5].

Absorption and fluorescence spectra were recorded with a Hitachi Nicolet Evolution 600 spectrophotometer and a Shimadzu RF-5301PC spectrofluorimeter.

We obtained the energy states of molecules by the method of partial neglect of differential overlap with spectroscopic parametrization [7] and calculated from them the spectra of electronic absorption from the ground and first excited ($S_1 \rightarrow S_n$) singlet and ($T_1 \rightarrow T_n$) triplet states. This method takes into account only electronic transitions between the zero vibrational levels of different electronic states and cannot be used to estimate the width of a vibronic band, which is determined by the interaction of the purely electronic transition with the vibrational levels of electronic states.

The lasing parameters of the dyes in solutions were studied upon transverse pumping by 12-ns, 30-mJ, 532-nm second-harmonic pulses and 12-ns, 34-mJ, 308-nm pulses from a XeCl laser. A single-mirror plane-parallel nonselective resonator was used, which was formed by an aluminium mirror and the face of a quartz cell with a laser dye solution. The active medium length in the cell was 1 cm and the resonator base was 1.5 cm. The output laser power was detected with an IMO-2N calorimeter and an ED-100-UV (Gentec EO) pyroelectric sensor. The laser emission spectra were recorded with a S100 (Solar LC) spectrometer. The scheme of the experimental setup for studying lasing parameters is described in detail in [8]. The lasing efficiencies of dyes emitting in different spectral ranges or pumped at different wavelengths were compared by measuring, apart from the energy lasing efficiency, the quantum lasing efficiency equal to the product of the energy efficiency by the energy ratio of pump and laser photons.

The excited-state absorption spectra were studied by the pump – probe method [1] by using the original setup with the nanosecond time resolution. The setup provides the integral detection of the optical density induced in a medium per pulse and allows the separation (by using an optical delay line) of the short-lived (during the pump pulse) and long-lived (more than 40 ns) induced absorptions. The scheme, the operation principle, and parameters of the setup are described in [9].

3. Results and discussion

3.1 Linear absorption and luminescence parameters

The absorption and fluorescence spectra of dyes 1 – 3 are presented in Fig. 2 and their absorption and luminescence parameters are listed in Table 1.

Figure 2 shows that dyes 1 and 2, which have broader and shorter-wavelength absorption bands than dye 3, well absorb radiation at a wavelength of 532 nm, whereas the extinction coefficient ε of dye 3 at this wavelength is almost an order of magnitude lower (Table 1), which should affect the lasing efficiency.

An important characteristic affecting lasing parameters is the overlap of the absorption and fluorescence spectra of dyes, which is determined by the Stokes shift and half-widths of absorption and fluorescence bands. The minimal overlap of the absorption and fluorescence spectra is observed for dye 2, while the maximum overlap is observed for dye 3. Despite the large Stokes shift, the absorption and fluorescence spectra of dye 1 are also strongly overlapped because the absorption band is very broad.

The quantum yield of fluorescence F_{fl} of dyes 1 – 3 lies in the range 0.15 – 0.28. The nonradiative relaxation in these dyes in solutions occurs due to internal conversion and photoisomerization [5, 6].

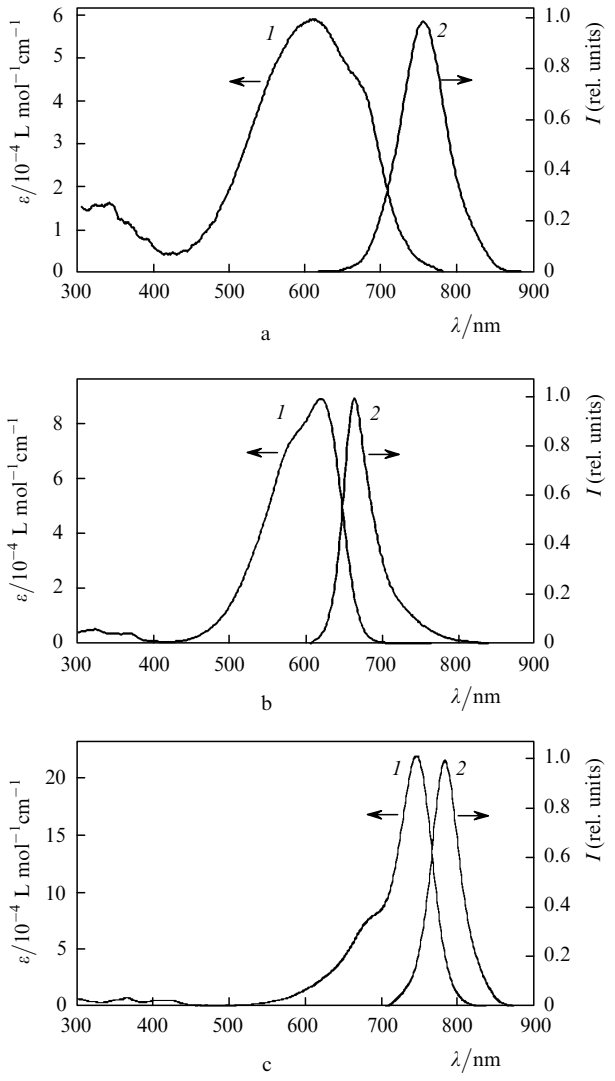

Figure 2. Absorption (*1*) and fluorescence (*2*) spectra of dyes 1 (a), 2 (b), and 3 (c) in PC solutions.

The positions of absorption and fluorescence bands observed in experiments correspond to calculations. The red shift of the experimental absorption and fluorescence bands with respect to the corresponding calculated bands can be explained by the influence of the solvent, which was neglected in calculations performed for purely electronic transitions in isolated molecules.

3.2 Excited-state absorption

Figure 3 presents experimental transient absorption spectra of the dyes excited by nanosecond laser pulses. The spectra are recorded in the range from 400 to 600 nm. The

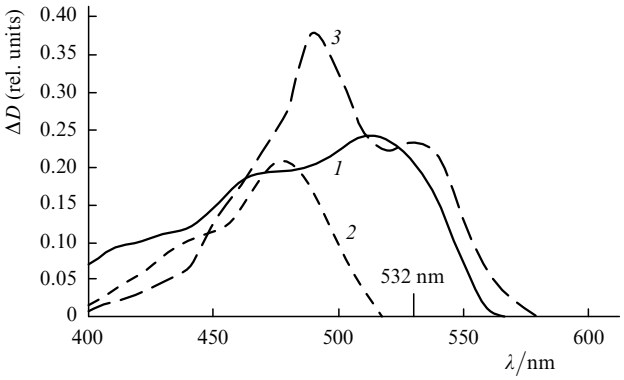

Figure 3. Transient nanosecond absorption spectra of dyes (ΔD is the optical density change). The time delay between pump and probe pulse is zero. Curves (*1*), (*2*), and (*3*) correspond to dyes 1, 2, and 3.

detection of transient absorption in the longer-wavelength region was complicated due to intense absorption from the ground state or fluorescence of the dyes. The curves presented in Fig. 3 correspond to the case when the time delay between the pump and probe pulse was absent (synchronous excitation and probing). For the time delay of 40 ns, ΔD is virtually zero. Therefore, the relaxation of the induced optical density occurs in the nanosecond range, and the observed absorption corresponds to the short-lived $S_1 \rightarrow S_n$ absorption.

The induced absorption spectrum for dye 2 coincides with the spectrum obtained for this molecule excited by picosecond pulses [10], which was also interpreted by the authors as the $S_1 \rightarrow S_n$ absorption.

The experimental data are confirmed by quantum-chemical calculations. The results of calculations of the $S_1 \rightarrow S_n$ absorption spectra in the range from 300 to 900 nm are presented in Table 2. The calculations are in good agreement with experiments (the discrepancy in the positions of absorption bands does not exceed 1000 cm^{-1}) in the range from 400 to 600 nm, where the induced absorption spectra were recorded.

Calculations also gave, additionally to experiments, the data about the $S_1 \rightarrow S_n$ absorption in regions with intense absorption from the ground state ($S_0 \rightarrow S_n$) and also in the fluorescence region of the dyes from 600 to 900 nm. According to calculations, the most intense $S_1 \rightarrow S_n$ transitions in all three molecules are located in the red spectral region and overlap with the long-wavelength $S_0 \rightarrow S_n$ absorption band of dye 1 or the fluorescence band of dyes 2 and 3. Table 2 shows that the $S_1 \rightarrow S_n$ absorption of dyes 1 and 3 in this spectral range is caused by one electronic transition ($S_1 \rightarrow S_4$ and $S_1 \rightarrow S_3$, respectively), while this absorption for dye 2 is caused by two transitions $S_1 \rightarrow S_2$ and $S_1 \rightarrow S_5$. The excited-state absorption in this

Table 1. Experimental (PC solvent) and calculated (isolated molecule) linear absorption and luminescence parameters of the dyes studied.

Dye	Absorption						Fluorescence				CC/nm
	λ_{abs}/nm		$\Delta\nu_{abs}$/cm^{-1}	$\varepsilon/10^{-4}$ L $mol^{-1}cm^{-1}$			λ_{fl}/nm		F_{fl}	$\Delta\nu_{fl}$/cm^{-1}	
	Experiment	Calculation	Experiment	λ_{max}/nm	532 nm	308 nm	Experiment	Calculation		Experiment	Experiment
1	610	592	4730	6	3.4	1.5	753	701	0.15	1240	143
2	620	545	3030	9	2.9	0.7	663	590	0.15	900	43
3	744	750	1020	22	0.3	0.7	782	754	0.28	740	38

Table 2. Experimental (PC solvent) and calculated (isolated molecule) data for the $S_1 - S_n$ absorption spectra of dyes 1–3.

Dye	Experiment	Calculation		
	λ_{abs}/nm	the $1 \rightarrow n$ transition	λ_{abs}/nm	f *
		$1 \rightarrow 49$	301	0.010
		$1 \rightarrow 32$	344	0.011
		$1 \rightarrow 26$	366	0.011
		$1 \rightarrow 25$	381	0.022
		$1 \rightarrow 24$	385	0.017
	430	$1 \rightarrow 16$	420	0.067
1	460	$1 \rightarrow 13$	451	0.020
		$1 \rightarrow 11$	475	0.010
	515	$1 \rightarrow 9$	488	0.084
		$1 \rightarrow 8$	508	0.024
		$1 \rightarrow 6$	536	0.024
		$1 \rightarrow 5$	550	0.013
		$1 \rightarrow 4$	586	1.220
		$1 \rightarrow 27$	337	0.036
		$1 \rightarrow 19$	390	0.047
	450	$1 \rightarrow 13$	466	0.016
2	478	$1 \rightarrow 12$	478	0.012
		$1 \rightarrow 7$	592	0.042
		$1 \rightarrow 5$	682	0.590
		$1 \rightarrow 2$	803	0.542
		$1 \rightarrow 29$	318	0.014
		$1 \rightarrow 15$	408	0.037
		$1 \rightarrow 13$	435	0.011
		$1 \rightarrow 11$	444	0.017
3	490	$1 \rightarrow 6$	512	0.240
	535	$1 \rightarrow 5$	568	0.018
		$1 \rightarrow 4$	629	0.012
		$1 \rightarrow 3$	634	1.018
		$1 \rightarrow 2$	856	0.038

Note: *the oscillator strength of an electronic transition.

region is mainly determined by the molecular orbitals (MOs) of dyes localised in the polymethine chain. The MOs of the end fragments are almost not involved in the formation of the $S_1 \rightarrow S_n$ absorption spectrum in the long-wavelength region.

The situation is different in the blue-green and UV spectral regions. In this case, along with the MO of the polymethine chain, the end fragments of dyes are also involved in the formation of the absorption spectrum. Thus, the $S_1 \rightarrow S_n$ absorption of dye 1 in the green spectral region, corresponding to the emission wavelength of a Nd:YAG laser, is formed by two electronic transitions $S_1 \rightarrow S_8$ and $S_1 \rightarrow S_9$ (Table 2) localised in the polymethine chain and in the indolinylidene fragment contained in all the dyes under study. The $S_1 \rightarrow S_{12}$ and $S_1 \rightarrow S_5$ electronic transitions in dyes 2 and 3, respectively, have the same localisation.

The formation of the shorter-wavelength region of the $S_1 \rightarrow S_n$ spectrum is determined, apart from MOs localised in the polymethine chain, by the cyano group of dye 2 (the $S_1 \rightarrow S_{19}$ transition), the phenyl rings of both end fragments in dye 1 the $S_1 \rightarrow S_{13}$ and $S_1 \rightarrow S_{16}$ transitions) and the phenyl rings of indolinylidene fragments in dye 3 (the $S_1 \rightarrow S_6$transition).

3.3 Lasing parameters

The lasing parameters of the dyes obtained in the study are presented in Table 3 and Fig. 4.

Table 3. Lasing parameters of polymethine dyes in PC solutions ($C = 10^{-3}$ M).

Dye	λ_{gen}/nm	Energy/quantum lasing efficiency (%)	
		$\lambda_{pump} = 308$ nm	$\lambda_{pump} = 532$ nm
1	794	20/51	36/54
2	720	12/28	46/62
3	845	12/33	5.7/9.1

Dye 1 in PC transversely pumped in a nonselective resonator by the second harmonic of a Nd:YAG laser generates laser radiation with the energy efficiency up to 36 %. The maximum lasing efficiency is achieved at the dye concentration 10^{-3} M. The lasing efficiency of symmetric dye 3 with the polymethine chain of the same length is only 5.7 %. For the convenience of comparison of the dependences of the lasing efficiency on the pump power density at different excitation wavelengths, the lasing efficiency for dye 3 pumped at 532 nm is presented at a scale magnified by six times [curve (*5*) in Fig. 4].

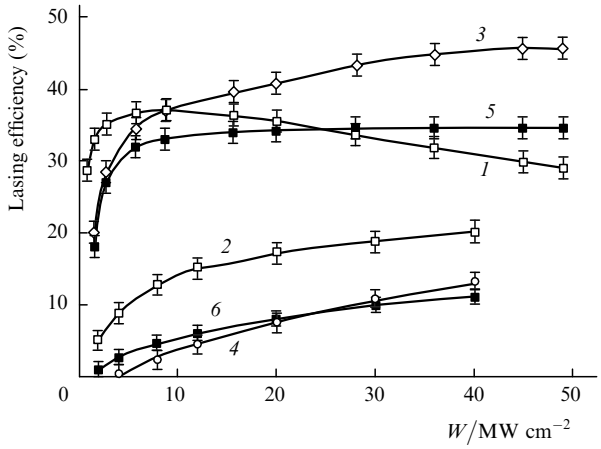

Figure 4. Dependences of the lasing efficiency on the pump power density for the solutions of dyes in PC, $C = 10^{-3}$ M [1: (*1*), (*2*); 2: (*3*), (*4*); 3: (*5*), (*6*)] upon excitation by the 532-nm second harmonic of a Nd:YAG laser (*1*, *3*, *5*) and by a XeCl laser at 308 nm (*2*, *4*, *6*). The ordinate for curve (*5*) is magnified by a factor of six.

The quantum lasing efficiency for dye 1 pumped at 532 nm achieves 54 %, whereas this efficiency for dye 3 is only 9.1 %. This large difference is first of all explained by the fact that dye 1 absorbs the pump radiation at 532 nm much stronger (see Fig. 2). The molar extinction coefficient ε of asymmetric dye 1 at 532 nm is 34 000 L mol^{-1}cm^{-1}, whereas this coefficient for symmetric polymethine dye 3 is only about 3000 L mol^{-1}cm^{-1}. Note that the increase in the concentration of dye 3 in solution does not result in the increase in the lasing efficiency because this dye has a small Stokes shift and narrow absorption and fluorescence bands, and for this reason the reabsorption of laser radiation considerably increases at high concentrations, thereby reducing the lasing efficiency.

Dye 3 emits laser radiation at a wavelength of 845 nm, whereas dye 1 emits laser radiation at 794 nm. However, because the fluorescence spectrum of asymmetric dye 1 is considerably broader (see Table 1) than that of symmetric polymethine dyes, the use of a tunable selective resonator makes it possible to obtain efficient lasing in dye 1 in a longer-wavelength region as well.

Despite the high lasing efficiency, dye 1 has one substantial disadvantage. Figure 4 shows the dependence of the lasing efficiency on the pump power density W. One can see that already for $W = 5 - 7$ MW cm^{-2}, the saturation of the lasing efficiency is observed, and as the pump power density is further increased, the lasing efficiency decreases [curve (*1*)]. This can be explained by losses appearing in the medium upon high-power laser pumping.

The decrease in the lasing efficiency can be caused, in particular, by the formation of a thermal lens [11] producing optical inhomogeneities in a medium. However, we discard this reason because excitation was performed by rather short pulses (12 ns). The dependences similar to curve (*1*) in Fig. 4 were observed for dye 1 pumped at 532 nm and also in other solvents with different thermal properties. At the same time, upon pumping at 308 nm (thermal losses in the medium in this case are considerably greater), no saturation of the lasing efficiency was observed [curve (*2*) in Fig. 4] and the laser beam quality was not deteriorated. In addition, the so-called two-passage superluminescence regime [12] is realised in the optical scheme used in our experiments, and thermooptic distortions upon nanosecond pumping should not affect the energy parameters of radiation, unlike the case of tunable dye lasers, in which complex resonators are used [13]. In our opinion, the experimental dependence of the lasing efficiency on the pump power is determined by excited-state absorption, which we will consider below.

The study of the lasing parameters of dye 1 pumped at 308 nm showed that the lasing efficiency of this dye pumped by UV radiation is high as well. The energy lasing efficiency was 20 % and the quantum lasing efficiency was 51 % (compared to 54 % for pumping at 532 nm). No rapid saturation of the lasing efficiency with increasing the UV pump power was observed [curve (*2*) in Fig. 4).

Dye 2 emits in the shorter-wavelength region (710–720 nm) compared to dye 1. The energy lasing efficiency upon pumping at 532 nm achieves 46 % (Fig. 3), the quantum lasing efficiency exceeding 60 % (Table 2). The lasing parameters of dye 2 are better than these for the known laser dye oxazine 1 emitting in the same spectral region.

Upon pumping by UV radiation at 308 nm, the lasing efficiency of dye 2 is lower, the maximum energy lasing efficiency being only 12 % (quantum efficiency is 28 %) at the concentration 10^{-3} M. This is explained first of all by a weak absorption of radiation by this dye at 308 nm ($\varepsilon =$ 7000 L mol^{-1}cm^{-1}, Table 1). As the dye concentration was increased up to 2×10^{-3} M, the lasing efficiency increased up to 19 %.

3.4 Influence of the excited-state $S_1 \rightarrow S_n$ absorption on lasing parameters

Let us analyse the influence of the excited-state singlet–singlet absorption on the lasing parameters of dyes 1–3. Consider the case of pumping by the 532-nm second harmonic of a Nd:YAG laser. The $S_1 \rightarrow S_n$ absorption cross sections of dyes 1 and 3 at 532 nm considerably exceed the ground-state $S_0 \rightarrow S_1$ absorption cross section at this wavelength. The $S_1 \rightarrow S_n$ absorption band of dye 2 is shifted to the blue and has a lower intensity (Fig. 3). It follows from calculations that singlet–singlet absorption for dyes 1 and 3 in the fluorescence region is weak, while dye 2 has intense $S_1 \rightarrow S_n$ absorption bands near the maximum of the fluorescence band (Table 2). Thus, dyes 1 and 3 have the excited-state absorption bands at the pump wavelength, while dye 2 – at the fluorescence wavelength.

The specific feature of dye 1 is the saturation of the lasing efficiency for $W < 10$ MW cm^{-2} and its further decrease with increasing W [curve (*1*) in Fig. 4]. In our opinion, this is caused by the intense singlet–singlet absorption of the pump radiation, which produces the efficient depletion of the upper laser level due to $S_1 \rightarrow S_n$ transitions. The saturation of the lasing efficiency for $W >$ 20 MW cm^{-2} was also observed for dye 3 [curve (*5*) in Fig. 4], which is also caused by the excited-state absorption of the pump radiation.

The difference in the dependences of the lasing efficiency on W is probably is related not only to the $S_1 \rightarrow S_n$ absorption, but also to the different intensities of linear absorption at the pump wavelength. Dye 1 has a broad absorption band (FWHM is 4730 cm^{-1}) and can be efficiently excited by the second harmonic of a Nd:YAG laser, the molar extinction coefficient of this dye at the pump wavelength being 34 000 L mol^{-1}cm^{-1}. The extinction coefficient of dye 3 (Fig. 2) with a narrow absorption band (FWHM is 1020 cm^{-1}) is only $\sim$ 3000 L mol^{-1}cm^{-1} at 532 nm. These dyes have comparable excited-sate lifetimes, while the S_1-state saturation intensities for them differ almost by an order of magnitude. Because the general absorption efficiency is proportional to the absorption cross section and the concentration of molecules at a particular level, the saturation of the lasing efficiency for the dye with a higher linear absorption occurs earlier for the same pump intensity, which we observed for dyes 1 and 3.

A small value of ε for dye 3 at the pump wavelength is the reason for a low lasing efficiency, which is approximately 6 times lower than these for dyes 1 and 2. The increase in the dye concentration above 10^{-3} M almost does not lead to the increase in the lasing efficiency. The influence of the ε value on the lasing efficiency for a series of symmetric carbocyanine dyes with different polymethine chain lengths was studied in detail in our paper [8].

The $S_1 \rightarrow S_n$ absorption in dye 2 at the pump wavelength, as pointed out above, is small, and the lasing efficiency continues to increase monotonically with increasing W up to 50 MW cm^{-2} [curve (*3*) in Fig. 4]. According to quantum-chemical calculations, the presence of the intense $S_1 \rightarrow S_n$ absorption in dye 2 in the fluorescence region almost does not affect the lasing efficiency but leads only (due to a broad fluorescence band) to the additional red shift of the laser emission spectrum in a nonselective resonator to a region where losses in the medium are small.

Upon pumping at 308-nm by a XeCl laser, the lasing efficiency of all the dyes increased with increasing the pump power in the range studied, which confirms the absence of considerable $S_1 \rightarrow S_n$ absorption at the pump wavelength, i.e. absorption with ε exceeding that for the ground-state absorption at this wavelength.

4. Conclusions

Our experimental and theoretical studies of cationic and intraionic polymethine dyes have shown that considerable $S_1 \rightarrow S_n$ absorption at the pump wavelength leads most likely to the decrease in their lasing efficiency with increasing pump powers producing a comparatively high population of the S_1 state. Thus, the lasing efficiency of dye 1, having a considerable $S_1 \rightarrow S_n$ absorption at the 532-nm

pump wavelength, saturates already for $W = 5 - 8$ MW cm^{-2}.

Unlike the $S_1 \rightarrow S_n$ absorption at the pump wavelength, such parasitic absorption at the emission wavelength of the dyes does not affect strongly the lasing efficiency, in our opinion, but leads, along with reabsorption, to the spectral region where the optimum between absorption losses in the medium and the gain is achieved. Therefore, by selecting dyes and pump sources, special attention should be paid to the $S_1 \rightarrow S_n$ absorption at the pump wavelength.

By using cationic asymmetric polymethine dyes of type 1, which have a broad absorption spectrum and efficiently absorb radiation at 532 nm, it seems promising to study the analogues of this dye with different end fragments, which are involved in the formation of the excited-state $S_1 \rightarrow S_n$ absorption spectra, and may provide higher lasing efficiencies.

Another method, which can reduce the influence of the $S_1 \rightarrow S_n$ absorption at the pump wavelength on the lasing efficiency at high pump powers, is the formation of the pump pulse of a specials shape. Such a pulse should consist of a prepulse of duration $3-5$ ns (the optimal duration depends on the spectral parameters of a particular dye) with a power density of ~ 1 MW cm^{-2}, which provides the development of lasing in the medium, considerably reducing the lifetime of the S_1 state due to simulated emission [14], and the main pulse with a high power density following immediately after the prepulse.

Acknowledgements. This work was partially supported by the Russian Foundation for Basic Research (Grant No. 07-02-00155-a).

References

1. Tkachenko N. *Optical Spectroscopy: Methods and Instrumentations* (Amsterdam: Elsevier B.V., 2006).
2. Zemskii V.I., Kolesnikov Yu.L., Meshkovskii I.K. *Fizika i tekhnika impul'snykh lazerov na krasitelyakh* (Physics and Technology of Pulsed Dye Lasers) (St. Petersburg: St. Petersburg State University, 2005).
3. Bokhan P.A., Buchanov V.V., Zakrevskii D.E., Kazaryan M.A., Kalugin M.M., Prokhorov A.M., Fateev N.V. *Lazernoe razdelenie izotopov v atomarnykh parakh* (Laser Isotope Separation in Atomic Vapours) (Moscow: Fizmatlit, 2004).
4. Carmichael I., Hug G. *J. Phys. Chem. Ref. Data*, **15**, 1 (1986).
5. Ishchenko A.A. *Stroenie i spektral'no-lyuminestsennye svoistva polimetinovykh krasitelei* (Structure and Absorption and Luminescence Properties of Polymethine Dyes) (Kiev: Naukova Dumka, 1994).
6. Ishchenko A.A., Kulinich A.V., Bondarev S.L., Knykshto V.N. *Opt. Spektrosk.*, **104**, 64 (2008).
7. Artyukhov V.Ya., Galeeva A.I. *Izv. Vyssh. Uchebn. Zaved., Ser. Fiz.*, **29**, 96 (1986).
8. Svetlicnyi V.A., Kopylova T.N., Maier G.V., Laoin I.N., Dervyanko N.A., Ishchenko A.A. *Kvantovaya Elektron.*, **37**, 118 (2007) [*Quantum Electron.*, **37**, 118 (2007)].
9. Savenkova N.S., Kuznetsova R.T., Lapin I.N., Svetlichnyi V.A., Mayer G.V., Shatunov P.A. *J. Mol. Structure*, **787**, 184 (2006).
10. Bondarev S.L., Tikhomirov S.A., Knyukshto V.N., Turban A.A., Ishchenko A.A., Kulinich A.V. *Opt. Spektrosk.*, **99**, 55 (2005).
11. Kuznetsova R.T., Kopylova T.N., Mayer G.V., Telminov E.N., Samsonova L.G., Svetlichnyi V.A., Sergeev A.K. *Proc. SPIE Int. Soc. Opt. Eng.*, **3403**, 186 (1998).
12. Schafer F.P. (Ed.) *Dye Lasers* (Berlin: Springer-Verlag, 1974; Moscow: Mir, 1976).
13. Levshin L.V., Saletskii A.M. *Lazery na osnove slozhnykh organicheskikh soedinenii* (Polyatomic Organic Compound Lasers) (Moscow: Moscow Sate University, 1992).
14. Svetlichnyi V.A., Filinov D.N., Lapin I.N. *Izv. Vyssh. Uchebn. Zaved., Ser. Fiz.*, **47**, 54 (2003).